Design and Demonstration of Compact and Broadband Wavelength Demultiplexer Based on Subwavelength Grating (SWG)

Fuling Wang, Xiao Xu, Chen Zhang, Chonglei Sun, and Jia Zhao

***Abstract*—An ultracompact and broadband silicon wavelength demultiplexer based on SWG-assisted directional coupler is designed and experimentally demonstrated for wavelength splitting of 1310 and 1550 nm. The embedded SWG enables significantly reduced footprint, due to the precise phase matching at 1550 nm and large phase mismatch at 1310 nm. As a result, the fabricated device has a length of only 9 μm, and provides high extinction ratios (ERs) of 23 dB and 19 dB at 1310 and 1550 nm, respectively. Its 3-dB bandwidths are 85 nm for O-band (ER $>$ 15 dB) and 140 nm for C-band (ER $>$ 10 dB).**

***Index Terms*—Directional coupler (DC), subwavelength grating (SWG), wavelength demultiplexer.**

I. Introduction

WAVELENGTH division multiplexing (WDM) is quite important to satisfy the continuously increasing demand of ultrahigh link capacity in optical communications [1]. Technology for separating and combining different wavelengths is fundamental to WDM system [2]. Integrated wavelength division demultiplexer is an essential block for building broad band services for Big data, large capacity communication and cloud computing applications, due to its advantages in device size and performances [3].

Much attentions have been given to demultiplexing wavelengths of 1310/1550 nm [4]–[6]. Conventional wavelength demultiplexers, such as diffraction grating couplers and micro-ring resonators exhibit small footprints and high extinction ratios, but their bandwidths are much narrow [7]–[9]. By comparison, the multimode interference (MMI) devices provide a relatively broad optical bandwidth and relax fabrication tolerance [10]–[12]. But, they usually have a relatively large length. In our previous work [13], subwavelength gratings are embedded in MMI to shrink the device footprint, yet the device length still exceeds thirty microns. Also, wavelength demultiplexer has been demonstrated using inverse design algorithm and the device footprint is 2.8×2.8 μm^2 [14]. Currently, most demultiplexers are assembled with the directional coupler (DC) thanks to its high extinction ratio and easy design process [15]–[18]. However, for wavelength demultiplexing, the device length is relatively long, because the coupling region length must be even multiples or odd multiples of the beat lengths for two wavelengths. Even though subwavelength grating structure is inserted in the coupling region of DC to adjust beat lengths, the total length of the wavelength demultiplexer is still up to tens of microns [19]. Moreover, the bandwidth of DC depends on the precise phase matching condition. Typically, the bandwidth is less than 40 nm [20]. Therefore, the demonstration of a compact wavelength demultiplexer with excellent performances is fairly desirable.

Recently, subwavelength gratings (SWGs) have been widely used to reduce the feature size, increase the bandwidth and relax the tolerance to fabrication imperfections [21]–[23]. SWGs are periodic structures that composed by interlaced segments of a high-refractive-index core material (e.g., Si) and a low-refractive-index cladding material (e.g., air or SiO_2), where the reflection and diffraction effects are suppressed by using a grating pitch that much smaller than the operating wavelength [24]–[26]. As a result, the SWG is denoted as a homogeneous medium with an equivalent refractive index, which presents the potential of providing a new degree of freedom for device design by manipulating structural parameters [27], [28]. Thus, it is a promising candidate for wavelength demultiplexer.

In this work, we design and experimentally demonstrate a wavelength demultiplexer that splits the wavelengths of 1310 nm and 1550 nm on a silicon-on-insulator (SOI) platform. In our design, one strip waveguide of the DC is replaced by a SWG waveguide. By optimally choosing the structural parameters of the SWG, its effective index is tuned carefully to satisfy the phase-matching condition at 1550 nm. Meanwhile, a large phase mismatch is maintained at 1310 nm. Therefore, the input light at 1310 nm propagates to the through port with negligible cross-coupling, while the light at 1550 nm is coupled to the adjacent SWG waveguide within one coupling length. Moreover, by employing the SWG configuration, the beat lengths are shortened substantially, resulting in the further reducing in device length. The fabricated device displays low insertion losses of less than 1.7 dB for both 1310 and 1550 nm, and provides high

Manuscript received February 15, 2022; accepted March 14, 2022. Date of publication March 16, 2022; date of current version April 11, 2022. This work was supported in part by the National Natural Science Foundation of China under Grant 62105183, in part by the Shandong Provincial Natural Science Foundation under Grant ZR2021QF052, in part by the National Key Research and Development Program of China under Grants 2018YFA0209000 and 2018YFB2200700, and in part by the Fundamental Research Funds of Shandong University. *(Corresponding author: Xiao Xu.)*

The authors are with the School of Information Science and Engineering, Shandong University, Qingdao 266237, China (e-mail: wangfulingsdu@163.com; xuxiao@sdu.edu.cn; chenzhang@sdu.edu.cn; chongleisun@sdu.edu.cn; zhaojia@sdu.edu.cn).

Digital Object Identifier 10.1109/JPHOT.2022.3160180

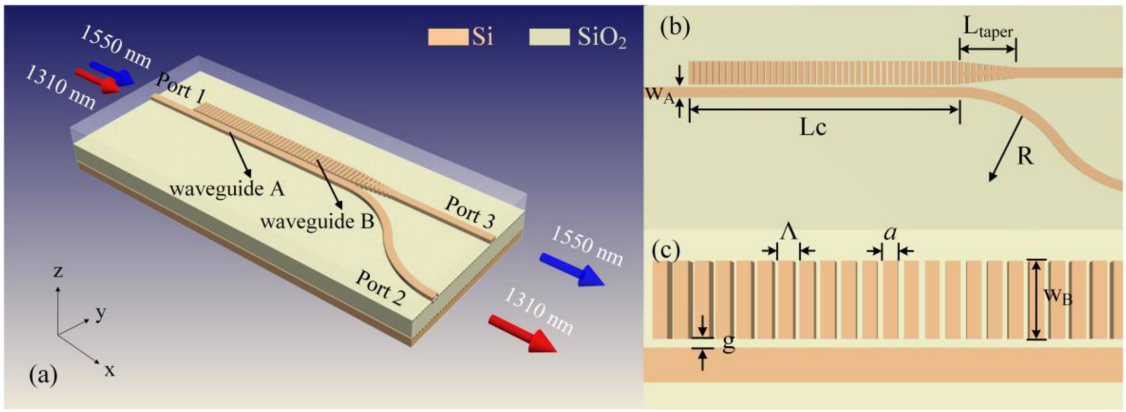

Fig. 1. (a) 3D schematic configuration of the designed wavelength demutiplexer. (b) Top view of the device. (c) Enlarged view of the coupling region.

extinction ratios (ERs) of 23 dB and 19 dB at 1310 and 1550 nm, respectively. Its 3-dB bandwidths are 85 nm for 1310 nm (ER $>$ 15 dB) and 140 nm for 1550 nm (ER $>$ 10 dB), which showing a broadband property that can cover almost the whole O-band and C-band. The total length of the present device is as short as 9 μm, which is about 10% of the traditional devices based on directional couplers, making this an ultracompact wavelength demultiplexer.

II. Structure and Operation Principle

The three-dimensional (3D) schematic of the proposed wavelength demultiplexer is illustrated in Fig. 1(a). The SOI platform with a 220 nm-thick top Si is implemented for our design which is buried in the SiO_2 cladding layer. The top view in Fig. 1(b) indicates the proposed wavelength demultiplexer mainly consisted by three parts: an input Si wire, a SWG-assisted asymmetrical directional coupler and two output wires. The asymmetrical DC section comprises a strip waveguide A, an evanescently coupled SWG waveguide B, and separated by a gap (g) of 100 nm. Within a consideration of the single-mode condition, width of strip waveguide A (w_A) is chosen to be 400 nm. A S-bend ($R =$ 15 μm) is attached to the strip waveguide A to decouple the two waveguides. As shown in Fig. 1(c), the periodic structure with Si and SiO_2 of SWG waveguide arranges along the direction of propagation with period of Λ. a and Λ-a represent the segment length of Si and SiO_2 in a period. To reduce the insertion loss, a SWG-strip transition is incorporated between the SWG waveguide B and output strip waveguide. The transition and the SWG waveguide B have the same period Λ and duty ratio a/Λ. In the subwavelength regime, the SWG waveguide period Λ is limited by the Bragg condition (Λ_{Bragg}). That is, the relation of Λ<$\Lambda_{Bragg} = \lambda/(2n_B)$ must be fulfilled, where n_B, the effective index of the SWG waveguide, can be deduced with certain w_B and n_{SWG}. Here, n_{SWG} represents the equivalent index of the SWG, which can be roughly estimated by the Rytov's formula [25]:

$$n_{SWG}^2 = \frac{a}{\Lambda} n_{Si}^2 + \frac{\Lambda - a}{\Lambda} n_{SiO_2}^2 \quad (1)$$

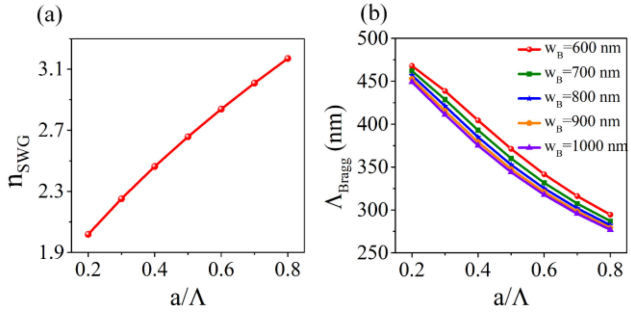

Fig. 2. (a) The equivalent index of SWG (n_{SWG}) with respect to duty ratio (a/Λ). (b) Bragg period length Λ_{Bragg} as a function of the duty ratio (a/Λ) for different waveguide width w_B.

where n_{Si} and n_{SiO2} are the indices of Si and SiO_2, respectively. The relationship between n_{SWG} and duty ratio is plotted in Fig. 2(a). For the wavelength of $\lambda_{min} = 1400$ nm, the Bragg period Λ_{Bragg} as a function of the duty ratio for different waveguide width w_B are depicted in Fig. 2(b). It reveals that, within the given ranges of waveguide width w_B and duty ratio, all the calculated Bragg period lengths are larger than 270 nm. Thus, the grating pitch Λ is fixed as 250 nm, which can be accepted in practical fabrication process.

For the wavelength demultiplexer based on conventional DC, two input wavelengths can be separated when the total length L is even multiples or odd multiples of the beat lengths for both wavelengths. Unfortunately, the beat lengths of 1310 and 1550 nm are much close, causing the lowest common multiple is large. Consequently, the total length of the wavelength demultiplexer based on conventional DC is too large. Instead, in our design, there is no need to fulfill the length relation in conventional DC. The operating principle can be explained as follows. By fine-tuning parameters of the SWG, the phase-matching condition is satisfied at 1550 nm, and a large phase mismatch is maintained at 1310 nm. Therefore, light at 1550 nm can be coupled to waveguide B effectively, while the coupling efficiency between these two waveguides at 1310 nm is dramatically frustrated because of the large phase mismatch. That is, $n^{1550}{}_A = n^{1550}{}_B$, at the same

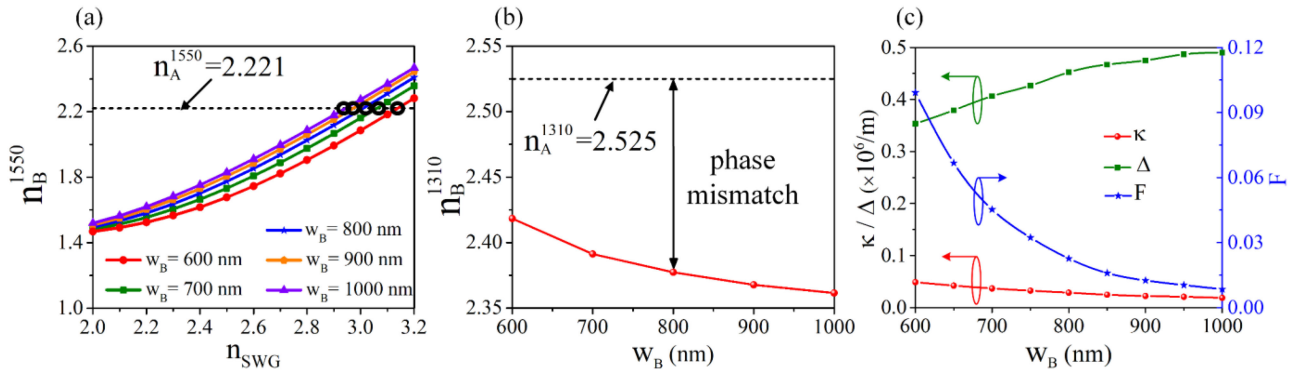

Fig. 3. (a) Variation of effective indices of the fundamental modes of strip waveguide A and SWG waveguide B with SWG refractive index n_{SWG} and waveguide width w_B at 1550 nm. (b) The phase mismatch at 1310 nm. (c) The coupling coefficient κ, the difference of the propagation constants $\triangle$ and the maximum power-coupling efficiency F as functions of waveguide width w_B at 1310 nm.

time, $n^{1310}{}_A \gg n^{1310}{}_B$. Consequently, when the total length is set to the coupling length of 1550 nm, 1550-nm light from port 1 can be coupled completely and transferred to the cross port 3, but light at 1310 nm can hardly couple and outputs from the through port 2. Unlike the conventional DC, the embedded SWG destroys the phase-matching condition at 1310 nm selectively, resulting in a short device length.

In designing the wavelength demultiplexer, the fundamental transverse electric (TE) modes are used as the input mode and output mode. According to the effective medium theory, the effective index can be deduced by 2D mode analysis. Accordingly, the SWG waveguide dimensions are determined. Specifically, we first calculated the refractive indices for waveguide A with $w_A = 400$ nm. The obtained refractive indices are 2.525 for 1310 nm ($n^{1310}{}_A$) and 2.221 for 1550 nm ($n^{1550}{}_A$). Here, the SWG waveguide B is treated as a homogenous medium with an equivalent index of n_{SWG}. The calculated effective indices of SWG waveguide B ($n^{1550}{}_B$) as functions of waveguide width w_B and equivalent refractive index n_{SWG} at 1550 nm are shown in Fig. 3(a). One can see that, for each width of w_B, there is a uniquely determined n_{SWG} to satisfy the precise phase matching condition. The corresponding results are illustrated as the black circle. For these specific w_B and n_{SWG}, the corresponding refractive indices at 1310 nm are calculated and illustrated in Fig. 3(b). It can be observed that the phase mismatch shows an upward trend as w_B increases. Meanwhile, the power-coupling efficiency at 1310 nm is also analyzed from a quantitative perspective. According to the coupled mode theory [29]–[31], the coupling coefficient between the two waveguides is related to the overlap integral of electromagnetic fields and can be calculated by the expression:

$$\kappa = \mathrm{i}\omega\varepsilon_0 \frac{\iint (n_B^2 - n_{SiO2}^2)\overrightarrow{E_{10}} \cdot \overrightarrow{E_{20}} dxdy}{\iint 2(\overrightarrow{E_{10}} \times \overrightarrow{H_{10}}) \cdot \overrightarrow{z}\, dxdy} \tag{2}$$

where ω represents an angular frequency of the electromagnetic fields, and ε_0 is the permittivity of material. E_{10} and H_{10} represent the electric and magnetic field of the fundamental mode in homogeneous SWG waveguide B. E_{20} represents the electric field of fundamental mode in strip waveguide A. F denotes the maximum power-coupling efficiency and is defined by:

$$F = \frac{\kappa^2}{\kappa^2 + \Delta^2} \tag{3}$$

Here we express the difference of the propagation constants between waveguides A and B as

$$\Delta = \frac{(\beta_1 - \beta_2)}{2} \tag{4}$$

where β_1 and β_2 are the propagation constants for the two lowest order modes. To ensure the phase mismatch condition at 1310 nm, $\triangle \gg \kappa$ should be satisfied.

The coupling coefficient κ, maximum power-coupling efficiency F and the difference of the propagation constants $\triangle$ as functions of waveguide width w_B are shown in Fig. 3(c). It can be observed that κ decreases and $\triangle$ increases with w_B. As a result, the difference between $\triangle$ and κ is increasing. When $w_B = 900$ nm, $\triangle$ is 0.475 $\times 10^6$/m, which is an order of magnitude larger than κ ($\kappa = 0.0223 \times 10^6$/m). Namely, only 1.2% of the total power at most can be coupled to the neighboring waveguide, which can be ignored reasonably.

Although κ decreases and Δ increases with the increment of w_B, the corresponding n_{SWG} and duty ratio are also increasing. Namely, the segment length of SiO_2 decreases, which puts higher requirement on the fabrication process. As the tradeoff between higher ER and ease fabrication, w_B is set to 900 nm finally. Therefore, n_{SWG} is 2.975 to satisfy the phase match condition for the 1550 nm according to results in Fig. 3(a). From Eq. 1, the theoretical value of a is 169 nm, namely, SiO_2 segment length Λ-a is 81 nm. The coupling length should be equal to the beat length of 1550 nm, which can be estimated with the following formula by calculating the eigen modes in the coupling region [32]:

$$L_\pi = \frac{\lambda_0}{2(n_0 - n_1)} \tag{5}$$

where n_0 and n_1 are effective indices of the first and second mode in the coupling region at wavelength λ_0. To obtain accurate parameters and optimal performances, calculations are performed with 3D FDTD simulations. It should be noted that the optimized

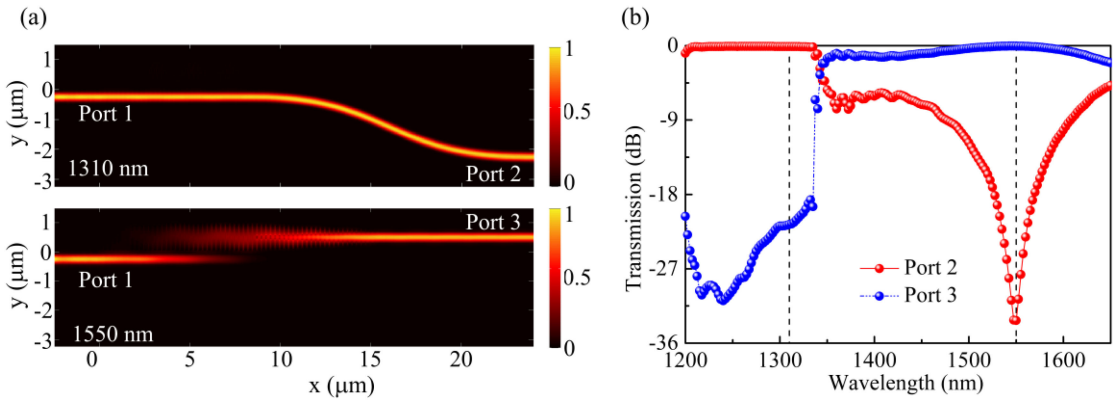

Fig. 4. (a) Field evolution for the central wavelengths of 1310 nm and 1550 nm through the demultiplexer. (b) Wavelength dependence of the demultiplexer.

TABLE I
DESIGN PARAMETERS OF THE WAVELENGTH DEMULTIPLEXER

Parameters	Symbol	Value
Top Si thickness	h	220 nm
Gap	g	100 nm
S-bent waveguide radius	R	15 μm
Strip waveguide width	w_A	400 nm
SWG waveguide width	w_B	900 nm
SWG pitch	Λ	250 nm
Si segment length	a	174 nm
SWG taper length	L_{taper}	6 μm
Coupling length	L_c	9 μm

silicon segment length is 174 nm and the corresponding duty cycle is 0.7. The beat length at 1550 nm determines the coupling length, which is only 9 μm. The detailed parameters of the device are summarized in Table I.

The transmission behaviors of the proposed demultiplexer, including the field evolution for wavelengths of 1310 nm and 1550 nm along the transmission direction are depicted in Fig. 4(a). The launched light at 1550 nm experiences a strong coupling along transmission direction and outputs from Port 3, while light at 1310 nm efficiently passes through the coupling region due to the large phase mismatch, and outputs from Port 2. As a result, the demultiplexing function for different wavelengths is well implemented. The performances of the proposed wavelength demultiplexer are assessed by the insertion loss (IL) and the extinction ratio (ER), which are defined as follows [5]:

$$IL = 10\log(P_d/P_{\text{in}}) \tag{6}$$

$$ER = 10\log(P_d/P_u) \tag{7}$$

Where P_{in} is the power in the input waveguide, P_d and P_u are the output powers from the desirable and undesirable output waveguides, respectively. Fig. 4(b) shows the wavelength response of Port 2 and Port 3, and calculated ILs and ERs are as follows: IL = 0.1dB and ER = 23.15 dB at 1310 nm; IL = 0.05 dB and ER = 32.94 dB at 1550 nm. For 1310 nm, the 3-dB bandwidth is broader than 135 nm (from 1200 nm to 1335 nm), in which the ERs are higher than 19 dB. For 1550 nm, in the range of C-band (from 1530 to 1565 nm), the ERs are also higher than 19 dB.

Furthermore, fabrication tolerances of structural dimensions are analyzed, and the results are shown in Fig. 5. The ER and IL as functions of width variation of strip waveguide A ($\triangle w_A$), SWG waveguide B ($\triangle w_B$), Si segment length ($\triangle a$), coupling region length ($\triangle L_c$), the thickness of top Si layer ($\triangle h$) and the gap ($\triangle g$) are demonstrated in Fig. 5(a)–(f), respectively. Here, the tolerances are characterized by the IL of lower than 0.5 dB and ER of higher than 10 dB. We can see that the tolerances on $\triangle w_A$ and $\triangle w_B$ are $\pm$ 8 nm and $\pm$ 40 nm, respectively. The performance of the designed device is less sensitive to $\triangle w_B$ for wider SWG waveguide is used. The tolerance on $\triangle a$ is $\pm$ 4 nm and the tolerance on $\triangle L_c$ is much larger with the range from -2 to 2 μm. Compared with $\triangle L_c$, the device is much vulnerable to $\triangle a$, and this happens because it manipulates the equivalent index greatly. The variation of $\triangle h$ is from -25 nm to 55 nm thanks to the less effect on TE mode. As for gap variation, $\triangle g$ can varies from -20 to 20 nm, mainly because the operating mechanism of the device is well kept within the gap range.

III. DEVICE FABRICATION AND CHARACTERIZATION

According to the theoretical analysis and design, we fabricated the wavelength demultiplexer using electron-beam lithography followed by plasma etching. The whole device was then covered with a SiO_2 layer as the top cladding. Scanning electron microscope (SEM) image is shown in Fig. 6. The fabricated device was measured using tunable O-band and C-band continuous wave lasers and power-meters. The measured scattering parameters for the compact WDM device are plotted in Fig. 7. The plotted wavelength range is limited by the tuning range of the tunable lasers in O-band and C-band.

The performance of the fabricated 1310/1550 nm wavelength demultiplexer was characterized of the wavelength from 1240 to 1380 nm, and from 1490 to 1630 nm, respectively. The measured transmission of the cross Port 3 and through Port 2 are

TABLE II
COMPARISON OF PERFORMANCES OF O-BAND/C-BAND WAVELENGTH DEMULTIPLEXERS REPORTED. (RESULT TYPE: EXPERIMENT)

References	Structure	Length (μm)	bandwidth (nm)		ER[a] (dB)		IL[b] (dB)	
			O-band	C-band	O-band	C-band	O-band	C-band
[4]	photonic crystal-MMI	108.5	74	103	32	20	3.8	0.7
[6]	MMI	117	/	80	13	10	5	5
[18]	DC	150	70	50	27	25.8	1	0.8
[14]	Inverse design– MMI	2.8	100	170	18	15	1.8	2.4
This work	**SWG-DC**	**9**	**85**	**140**	**23**	**19**	**1.7**	**1.4**

[a] ER shown here are the ERs at central wavelengths of O-band and C-band, respectively.
[b] IL shown here are the ILs at central wavelengths of O-band and C-band, respectively.

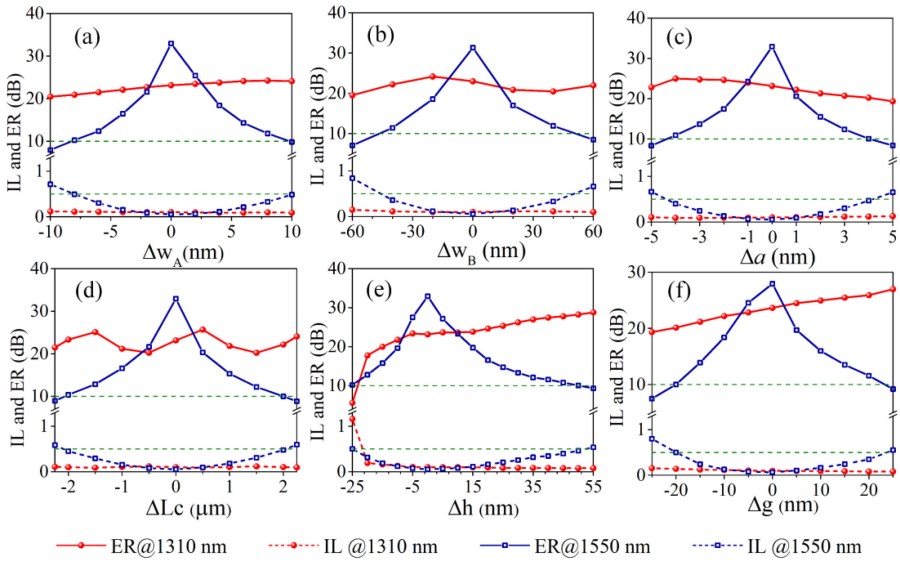

Fig. 5. ERs and ILs of the demultiplexer as functions of (a) the strip waveguide width ($\triangle w_A$), (b) SWG waveguide width ($\triangle w_B$), (c) the Si segment length ($\triangle a$), (d) coupling region length ($\triangle L_c$), (e) the thickness of top Si layer ($\triangle h$) and (f) the gap ($\triangle g$).

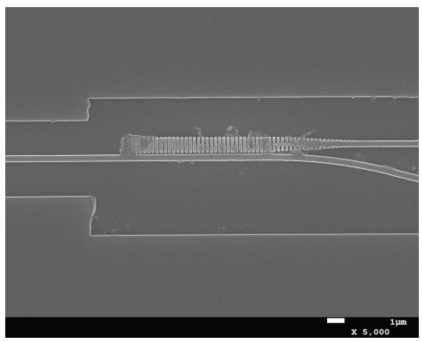

Fig. 6. SEM image of a fabricated wavelength demultiplexer.

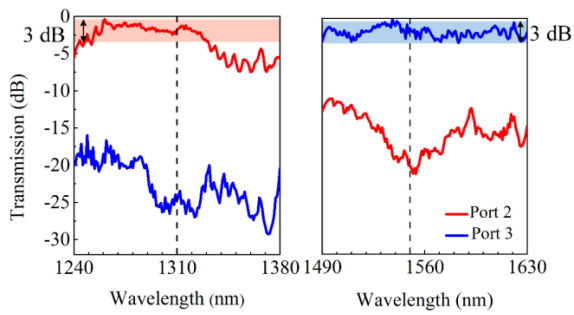

Fig. 7. The measured transmission spectra for the demultiplexer in the wavelength span of 1240-1380 nm and 1490-1630 nm. .

normalized to a strip waveguide with an input and an output grating coupler. Although somewhat degraded in performances with respect to the simulated results, the fabricated device exhibits a relatively low IL and high ER at the peak wavelength of 1310 nm and 1550 nm. At 1310 nm, the measured insertion loss is 1.7 dB, and the ER is 23 dB. The 3-dB bandwidth is as broad as 85 nm, and the ER is higher than 15 dB. As for 1550 nm, the measured IL and ER are 1.4 dB and 19 dB, respectively. The 3-dB bandwidth is 140 nm, which is limited by the source band, and the ER is higher than 10 dB within the whole test band.

Moreover, in the range of C-band (1530-1565 nm), the ER is higher than 16 dB. We attribute the performance deterioration of the fabricated device compared with the simulation results to fabrication imperfections.

The comparison of performances between the previously reported O-band/C-band wavelength demultiplexers and our work is summarized in Table II. By comparison, the proposed device shows competitive performances in easy design, compact footprint, broad bandwidth and high ER.

IV. Conclusion

In conclusion, we designed and experimentally demonstrated an ultracompact and broadband 1310/1550 nm wavelength demultiplexer by utilizing SWG-assisted asymmetrical directional coupler. The embedded SWG enables significantly reduced footprint, due to the precise phase matching at 1550 nm and large phase mismatch at 1310 nm. Therefore, the input light at 1310 nm propagates to the through port with negligible cross-coupling, while the light at 1550 nm is coupled to the adjacent SWG waveguide within one coupling length and an ultracompact footprint with the total length of 9 μm is obtained. The fabricated device displays low insertion losses of less than 1.7 dB for both 1310 and 1550 nm, and provides high extinction ratios (ERs) of 23 dB and 19 dB at 1310 and 1550 nm, respectively. Its 3-dB bandwidths are 85 nm for 1310 nm (ER $>$ 15 dB) and 140 nm for 1550 nm (ER $>$ 10 dB), which showing a broadband property that can cover almost the whole O-band and C-band. Our results imply that the proposed device is promising for high-efficiency wavelength demultiplexing with compact footprint and broad bandwidth.

References

[1] A. Liu *et al.*, "Wavelength division multiplexing based photonic integrated circuits on silicon-on-insulator platform," *IEEE J. Sel. Top. Quant. Electron.*, vol. 16, no. 1, pp. 23–32, Jan./Feb. 2010, doi: 10.1109/JSTQE.2009.2033454.

[2] C. A. Brackett, "Dense wavelength division multiplexing networks: Principles and applications," *IEEE J. Sel. Areas Commun.*, vol. 8, no. 6, pp. 948–964, Aug. 1990, doi: 10.1109/49.57798.

[3] B. Mukherjee, "WDM optical communication networks: Progress and challenges," *IEEE J. Sel. Areas Commun.,* vol. 18, no. 10, pp. 1810–1824, Oct. 2000, doi: 10.1109/49.887904.

[4] L. Xu *et al.*, "Broadband 1310/1550 nm wavelength demultiplexer based on a multimode interference coupler with tapered internal photonic crystal for the silicon-on-insulator platform," *Opt. Lett.*, vol. 44, no. 7, pp. 1770–1773, Apr. 2019, doi: 10.1364/OL.44.001770.

[5] Y. Shi, S. Anand, and S. He, "A polarization-insensitive 1310/1550-nm demultiplexer based on sandwiched multimode interference waveguides," *IEEE Photon. Technol. Lett.*, vol. 19, no. 22, pp. 1789–1791, Nov. 2007, doi: 10.1109/LPT.2007.906836.

[6] H. Yi, Y. Huang, X. Wang, and Z. Zhou, "Ultra-short silicon MMI duplexer," *Proc. SPIE*, vol. 8564, Nov. 2012, Art. no. 856410, doi: 10.1117/12.2001224.

[7] G. Roelkens, D. Van Thourhout, and R. Baets, "Silicon-on-insulator ultra-compact duplexer based on a diffractive grating structure," *Opt. Exp.*, vol. 15, no. 16, pp. 10091–10096, Jul. 2007, doi: 10.1364/OE.15.010091.

[8] C. R. Doerr, L. Chen, M. S. Rasras, Y. K. Chen, J. S. Weiner, and M. P. Earnshaw, "Diplexer with integrated filters and photodetector in Ge-Si using Γ-X and Γ-M directions in a grating coupler," *IEEE Photon. Technol. Lett.*, vol. 21, no. 22, pp. 1698–1700, Nov. 2009, doi: 10.1109/LPT.2009.2031820.

[9] L. Xu *et al.*, "Colorless optical network unit based on silicon photonic components for WDM PON," *IEEE Photon. Technol. Lett.*, vol. 24, no. 16, pp. 1372–1374, Aug. 2012, doi: 10.1109/LPT.2012.2204241.

[10] J. Xiao, X. Liu, and X. Sun, "Design of an ultracompact MMI wavelength demultiplexer in slot waveguide structures," *Opt. Exp.*, vol. 15, no. 13, pp. 8300–8308, Jun. 2007, doi: 10.1364/OE.15.008300.

[11] M. H. Ibrahim, S. Y. Lee, M. K. Chin, N. M. Kassim, and A. B. Mohammad, "Multimode interference wavelength multi/demultiplexer for 1310 and 1550 nm operation based on BCB 4024-40 photodefinable polymer," *Opt. Commun.*, vol. 273, no. 2, pp. 383–388, May 2007, doi: 10.1016/j.optcom.2007.01.006.

[12] S. L. Tsao, H. C. Guo, and C. W. Tsai, "A novel 1×2 single-mode 1300/1550 nm wavelength division multiplexer with output facet-tilted MMI waveguide," *Opt. Commun.*, vol. 232, no. 1-6, pp. 371–379, Mar. 2004, doi: 10.1016/j.optcom.2003.12.082.

[13] F. Wang, X. Xu, C. Sun, and J. Zhao, "Ultracompact 1310/1550 nm wavelength demultiplexer based on subwavelength grating-assisted multimode interference coupler," *Opt. Eng.*, vol. 60, no. 8, Aug. 2021, Art. no. 087104, doi: 10.1117/1.oe.60.8.087104.

[14] A. Y. Piggott, J. Lu, K. G. Lagoudakis, J. Petykiewicz, T. M. Babinec, and J. Vuckovic, "Inverse design and demonstration of a compact and broadband on-chip wavelength demultiplexer," *Nat. Photon.*, vol. 9, no. 6, pp. 374–377, May 2015, doi: 10.1038/nphoton.2015.69.

[15] J. Chen and Y. Shi, "An ultracompact silicon triplexer based on cascaded bent directional couplers," *J. Lightw. Technol.*, vol. 35, no. 23, pp. 5260–5264, Dec. 2017, doi: 10.1109/JLT.2017.2771214.

[16] J. Chen, L. Liu, and Y. Shi, "A polarization-insensitive dual-wavelength multiplexer based on bent directional couplers," *IEEE Photon. Technol. Lett.*, vol. 29, no. 22, pp. 1975–1978, Nov. 2017, doi: 10.1109/LPT.2017.2758019.

[17] B. Ni and J. Xiao, "Ultracompact silicon-based wavelength diplexer for 155/2 μm using subwavelength gratings," *Opt. Lett.*, vol. 44, no. 11, pp. 2775–2778, Jun. 2019, doi: 10.1364/OL.44.002775.

[18] H. Xu and Y. Shi, "On-chip silicon triplexer based on asymmetrical directional couplers," *IEEE Photon. Technol. Lett.*, vol. 29, no. 15, pp. 1265–1268, Aug. 2017, doi: 10.1109/LPT.2017.2721738.

[19] J. Chen, "A broadband wavelength demultiplexer assisted by SWG-based directional couplers," *Optik*, vol. 202, Feb. 2020, Art. no. 163602, doi: 10.1016/j.ijleo.2019.163602.

[20] Y. Shi, S. Anand, and S. He, "Design of a polarization insensitive triplexer using directional couplers based on submicron silicon rib waveguides," *J. Lightw. Technol.*, vol. 27, no. 11, pp. 1443–1447, Jun. 2009, doi: 10.1109/JLT.2008.2010465.

[21] Y. Wang *et al.*, "Compact broadband directional couplers using subwavelength gratings," *IEEE Photon. J.*, vol. 8, no. 3, Jun. 2016, Art. no. 7101408, doi: 10.1109/jphot.2016.2574335.

[22] L. Liu, Q. Deng, and Z. Zhou, "An ultra-compact wavelength diplexer engineered by subwavelength grating," *IEEE Photon . Technol. Lett .*, vol. 29, no. 22, pp. 1927–1930, Nov. 2017, doi: 10.1109/LPT.2017.2743109.

[23] L. Liu and Z. Zhou, "Subwavelength grating devices for optical on-chip multiplexing," *Proc. SPIE*, vol. 10823, Oct. 2018, Art. no. 108230A1-7, doi: 10.1117/12.2503322.

[24] P. Cheben, R. Halir, J. H. Schmid, H. A. Atwater, and D. R. Smith, "Subwavelength integrated photonics," *Nature*, vol. 560, no. 7720, pp. 565–572, Aug. 2018, doi: 10.1038/s41586-018-0421-7.

[25] S. Rytov, "Electromagnetic properties of a finely stratified medium," *Sov. Phys. JETP.*, vol. 2, pp. 466–475, 1956.

[26] M. W. Farn, "Binary gratings with increased efficiency," *Appl. Opt.*, vol. 31, no. 22, pp. 4453–4458, Aug. 1992, doi: 10.1364/AO.31.004453.

[27] R. Halir *et al.*, "Subwavelength-grating metamaterial structures for silicon photonic devices," *Proc. IEEE*, vol. 106, no. 12, pp. 2144–2157, Aug. 2018, doi: 10.1109/JPROC.2018.2851614.

[28] L. Sun, Y. Zhang, Y. He, H. Wang, and Y. Su, "Subwavelength structured silicon waveguides and photonic devices," *Nanophotonics*, vol. 9, no. 6, pp. 1321–1340, May 2020, doi: 10.1515/nanoph-2020-0070.

[29] L. Li, "Formulation and comparison of two recursive matrix algorithms for modeling layered diffraction gratings," *J. Opt. Soc. Amer. A*, vol. 13, no. 5, pp. 1024–1035, May 1996, doi: 10.1364/JOSAA.13.001024.

[30] R. Wang, L. Han, J. Mu, and W. Huang, "Simulation of waveguide crossings and corners with complex mode-matching method," *J. Lightw. Technol.*, vol. 30, no. 12, pp. 1795–1801, Feb. 2012, doi: 10.1109/JLT.2012.2187325.

[31] K. Okamoto, " Coupled mode theory," in *Fundamentals of Optical Waveguides*, 3rd ed. Amsterdam, The Netherlands: Elsevier, 2021.

[32] J. Donnelly, H. Haus, and N. Whitaker, "Symmetric three-guide optical coupler with nonidentical center and outside guides," *IEEE J. Quantum Electron.*, vol. QE-23, no. 4, pp. 401–406, Apr. 1987, doi: 10.1109/JQE.1987.1073370.